

Supplementary information

A Y₁ receptor ligand synergized with P-glycoprotein inhibitor improves therapeutic efficacy of multidrug resistant breast cancer

Yinjie Wang ^{‡, a, c}, Zhenqi Jiang ^{‡, a, c}, Bo Yuan ^a, Yuchen Tian ^a, Lingchao Xiang ^a, Yanying Li ^{a, c}, Yong Yang ^b, Juan Li ^{*, a}, Aiguo Wu ^{*, a}

^a Cixi Institute of Biomedical Engineering, CAS Key Laboratory of Magnetic Materials and Devices, & Key Laboratory of Additive Manufacturing Materials of Zhejiang Province, Ningbo Institute of Materials Technology and Engineering, Chinese Academy of Sciences, Ningbo 315201, P.R. China

^b Department of Clinical Laboratory, the Affiliated Hospital of Medical School of Ningbo University, Ningbo University School of Medicine, Ningbo, 315010, China

^c University of Chinese Academy of Sciences, Beijing 100049, China

Email: aiguo@nimte.ac.cn
lij@nimte.ac.cn

[‡] These authors contributed equally.

ESI Update: This file replaces the original version published on 27/08/2019

Keywords: multidrug resistant breast cancer, P-glycoprotein inhibitor, Y₁ receptor ligand, targeted therapy, nanomicelles

Materials: Ethanol, 1-ethyl-3-(3-dimethylaminopropyl) carbodiimide hydrochloride (EDAC), N-hydroxysuccinimide (NHS), 3-(4,5-dimethylthiazol-2-yl)-2,5 diphenyl-tetrazolium bromide (MTT), HPLC grade acetonitrile and trifluoroacetic acid (TFA) were purchased from Aladdin Industrial Inc (Shanghai, China). Penicillin, and streptomycin were purchased from Invitrogen™ (Carlsbad, USA). [Asn⁶, Pro³⁴]-NPY (AP) (YPSKPNNGEDAPAEDLARYYSALRHYINLITRPRY-NH₂) were synthesized by the Dechi Biosciences Co, Ltd (Shanghai, China). Doxorubicin (DOX) hydrochloride and IRDye780 iodide were purchased from Sigma-Aldrich Co. LLC (Shanghai, China). Tariquidar (Tar) was purchased from ApixBio (Hangzhou, China). DPSE-PEG2000 (50:50) and PLGA-PEG-2000 (50:50) were purchased from A.V.T. Pharmaceutical Ltd. (Shanghai, China). All reagents were used as received.

Characterization: Particle size, size distribution, and zeta potential of the nanomicelle dispersions were measured at room temperature by dynamic light scattering (DLS) using a Zeta particle size analyzer (Nano-ZS, Malvern, England). The data was collected on an autocorrelator with a detection angle of 173°. To obtain detailed structural and morphological information, ~1 µL of the diluted micelle dispersion was dropped onto a copper grid coated with a thin layer of carbon film and then dried at room temperature. High-resolution transmission electron microscopy (HRTEM) images were recorded from a JEOL-2100 (JEOL, Japan) instrument, which was operated at 200 kV.

Cell culture: Human multidrug resistant breast cancer line MCF-7/ADR was cultured in Dulbecco's modified Eagle's medium (DMEM). The medium contains fetal bovine serum (FBS, 20 wt %), penicillin (100 units/mL), and streptomycin (100 mg/mL). The cells were maintained in a 37 °C incubator with 5 % CO₂. Origin cells human breast cancer cells MCF-7 were bought from the Cell Bank of the Chinese Academy of Sciences (Shanghai, China), then incubated into MCF-7/ADR cell line in our lab ¹.

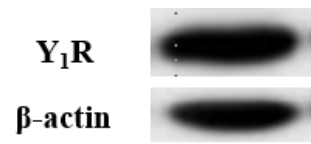


Figure S1 Western blot analysis of Y₁R expression on MCF-7/ADR cells.

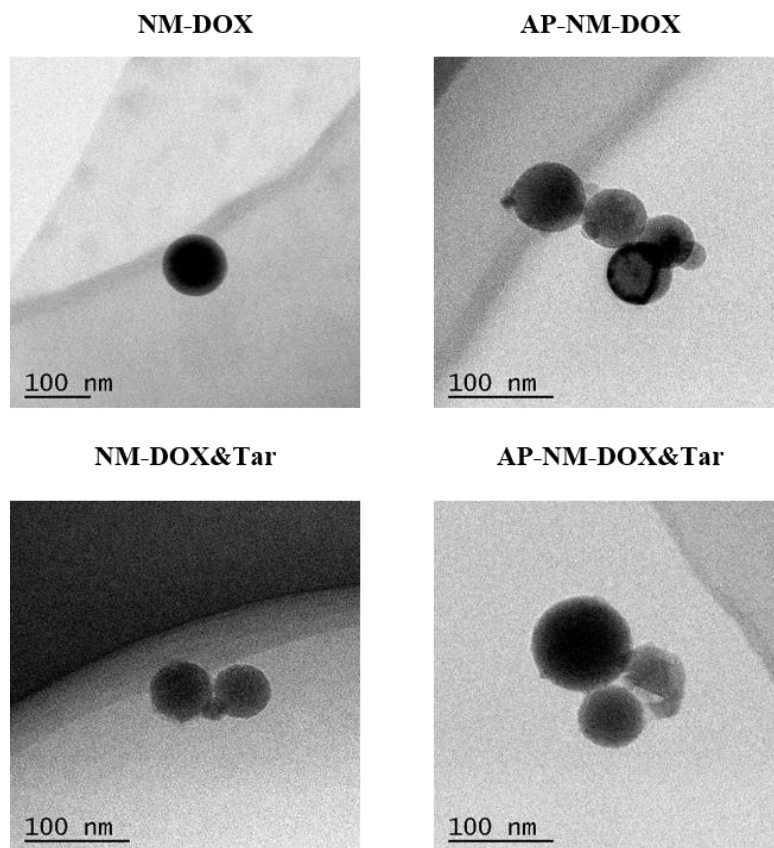


Figure S2 TEM images of NM-DOX, AP-NM-DOX, NM-DOX&Tar and AP-NM-DOX&Tar.

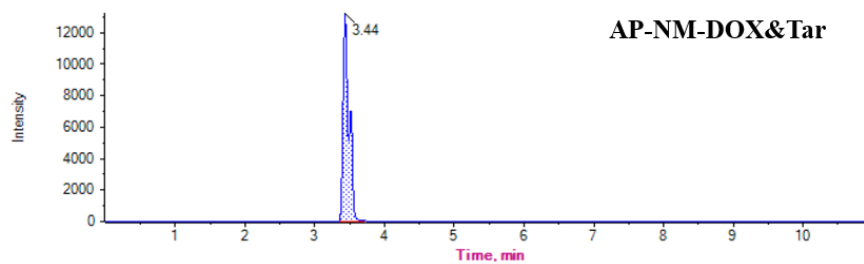
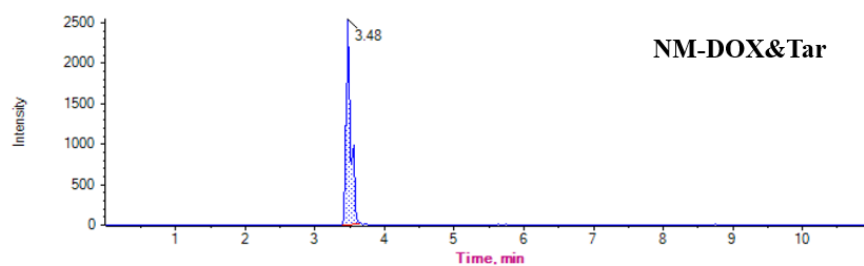
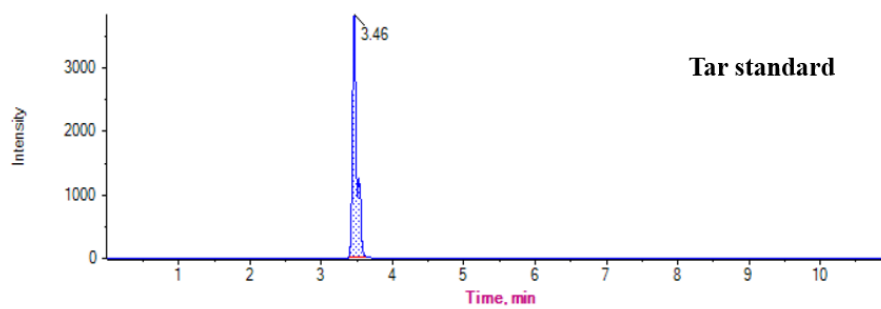


Figure S3 LC-MS images of Tar standards, NM-DOX&Tar and AP-NM-DOX&Tar.

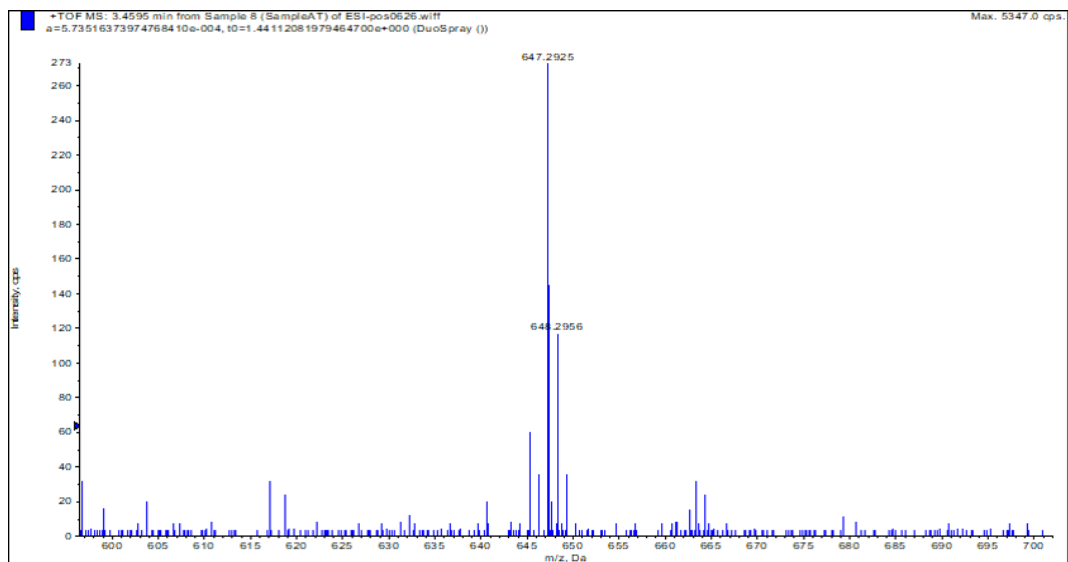


Figure S4 Mass spectrometry images of Tar.

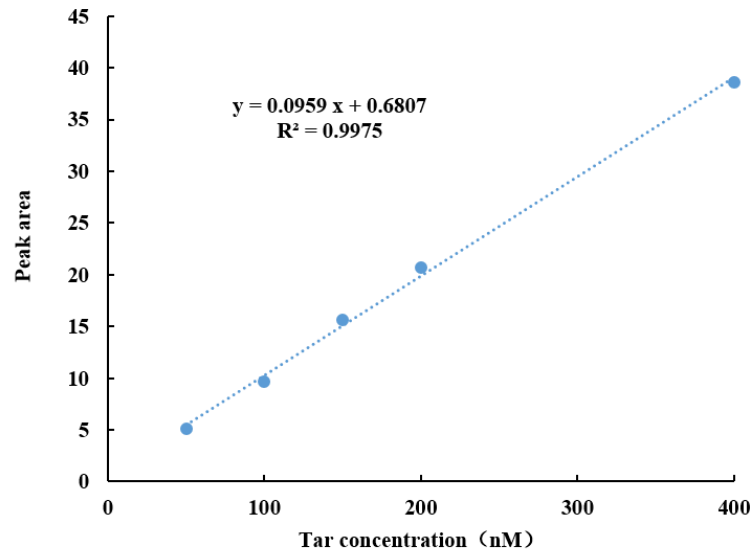


Figure S5 Standard curve of Tar. Tar concentration is varied from 50 to 400 nM.

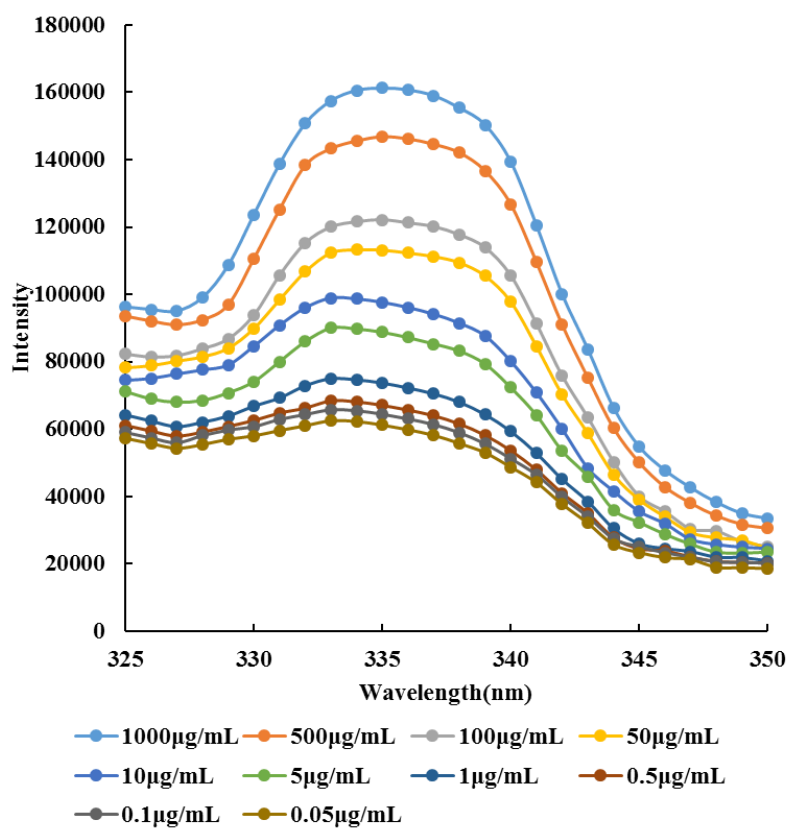


Figure S6 Pyrene excitation spectra of PEG-PLGA in aqueous solution. Emission wavelength is at 302 nm.

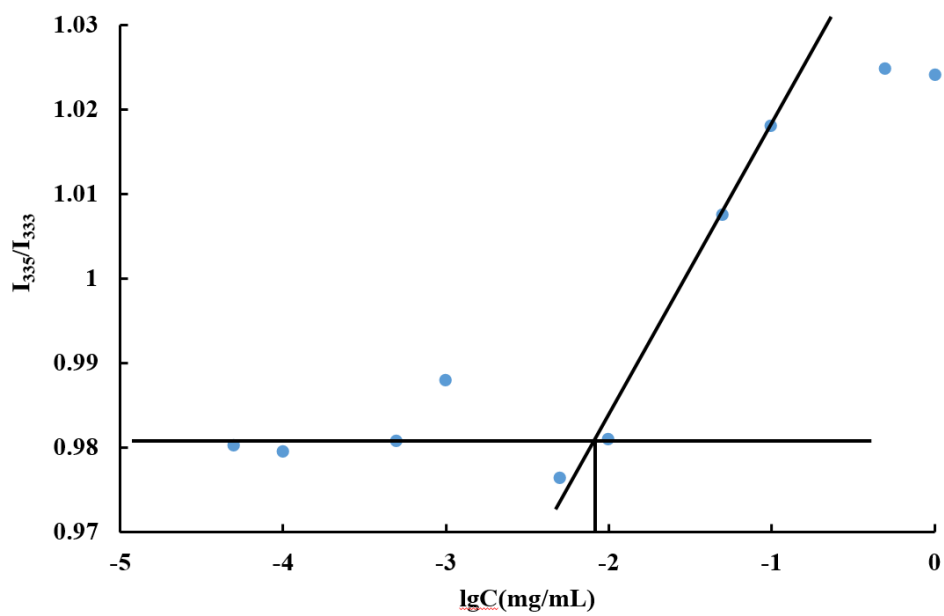


Figure S7 Intensity ratio of I_{335}/I_{333} versus $\lg C$ for PEG-PLGA in water. The critical micelle concentration of PEG-PLGA is $8.073 \mu\text{g/mL}$.

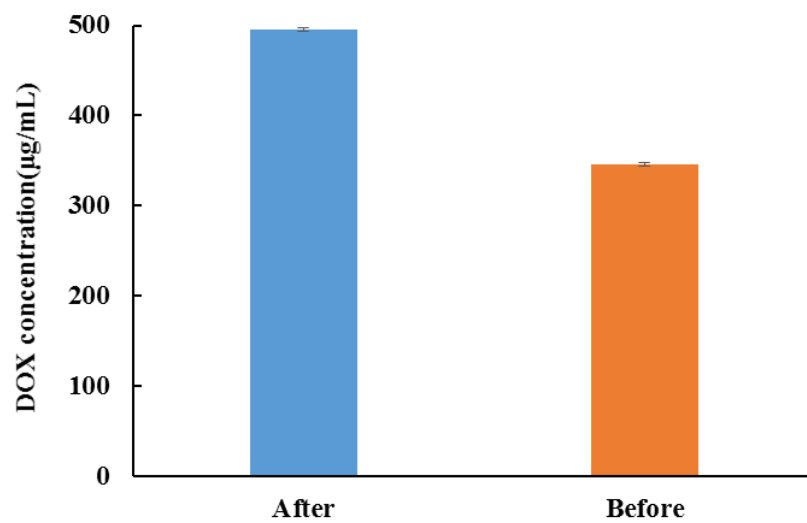


Figure S8 DOX concentration of AP-NM-DOX before and after the demulsification by acetonitrile.

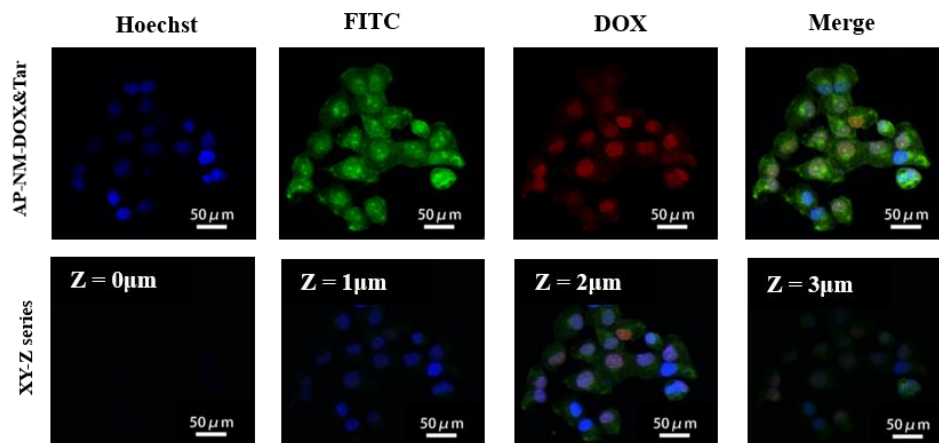


Figure S9 XY-Z series of MCF-7/ADR cells incubated with AP-NM-DOX&Tar for 8 h. Z-axis is from 0 to 3 μm.

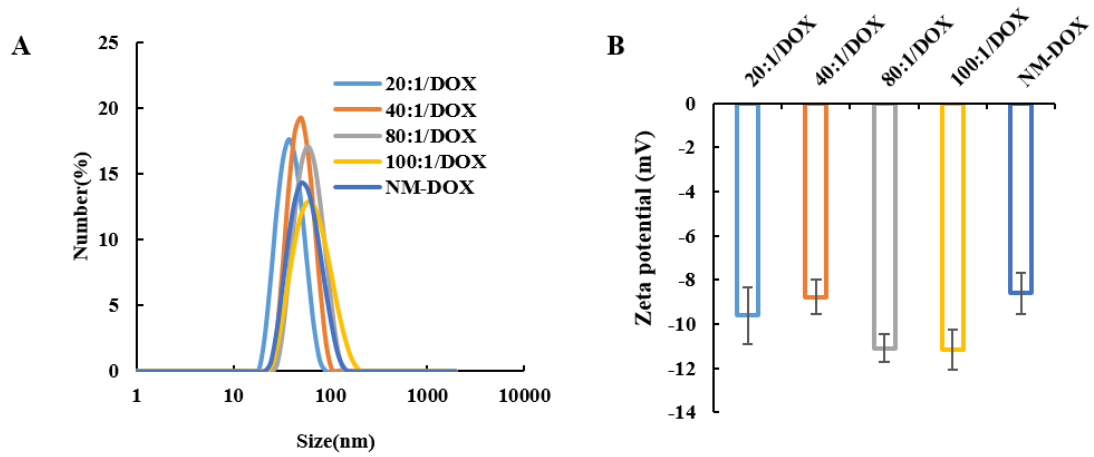


Figure S10 Effect of different proportions of PEG-PLGA to AP-DSPE-PEG (w/w) on particle size and zeta potential. The proportion of PEG-PLGA to AP-DSPE-PEG (w/w) varies from 20:1 to 100:1. Mean \pm SD (n = 3).

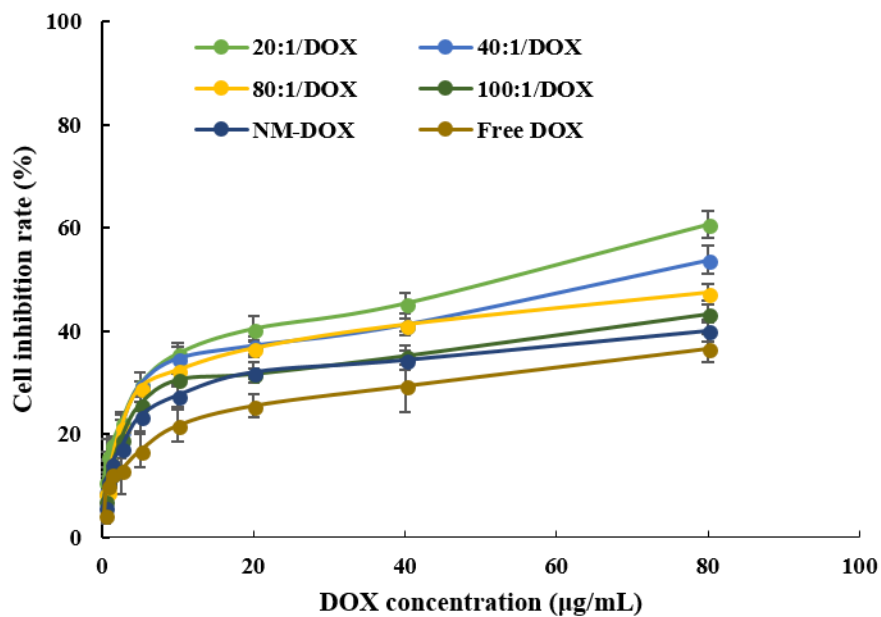


Figure S11 Inhibitory effect of different proportions of PEG-PLGA to AP-DSPE-PEG (*w/w*) on MCF-7/ADR cells. The proportion of PEG-PLGA to AP-DSPE-PEG (*w/w*) varies from 20:1 to 100:1. DOX concentration is varied from 0.3125 to 80 µg/mL. Mean ± SD (n = 3).

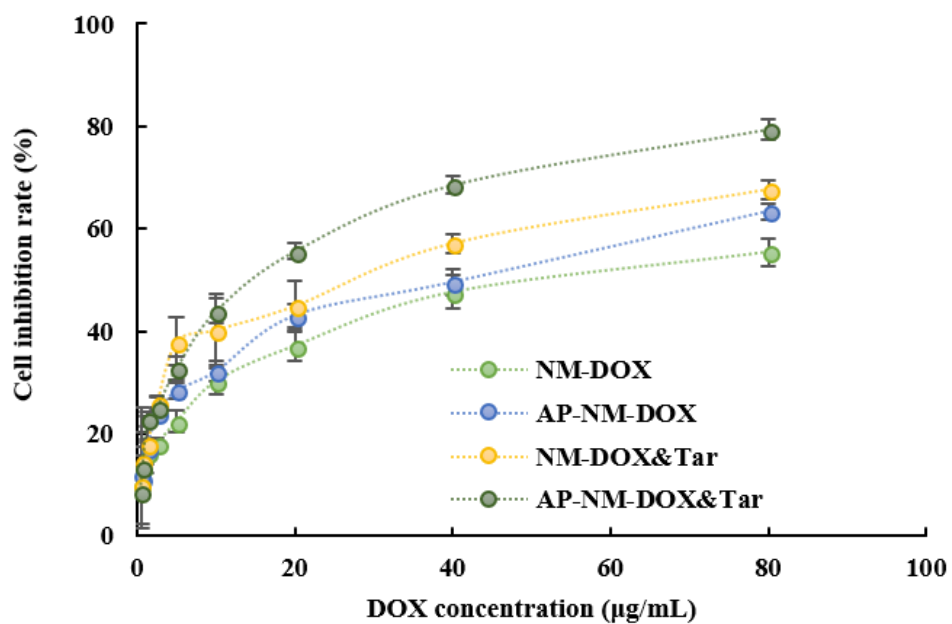


Figure S12 Inhibition effect of NM-DOX, AP-NM-DOX, NM-DOX&Tar, and AP-NM-DOX&Tar on MCF-7/ADR cells after 24 h incubation. DOX concentration is varied from 0.3125 to 80 µg/mL. Mean ± SD (n = 3).

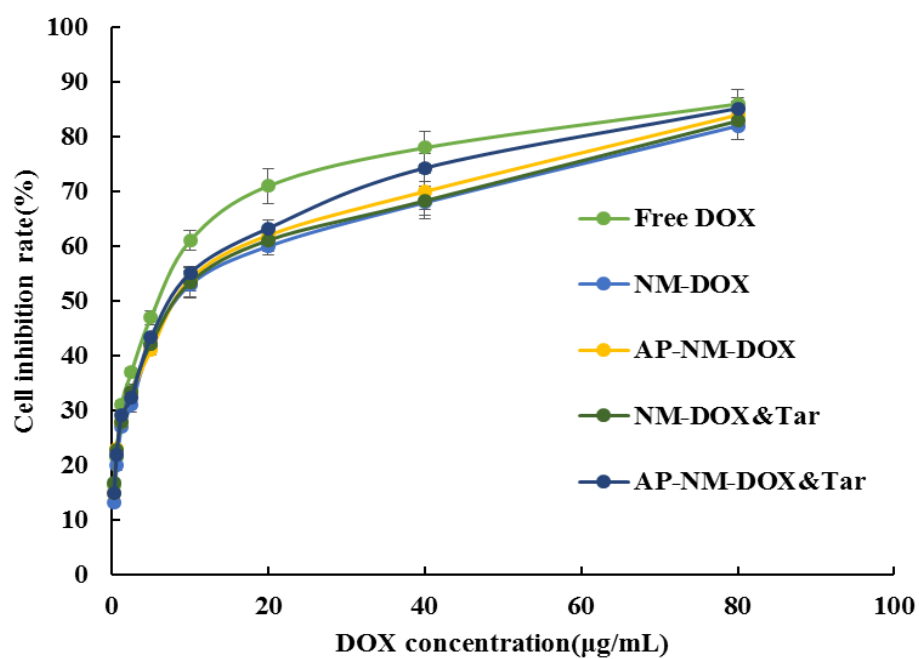


Figure S13 Inhibition effect of NM-DOX, AP-NM-DOX, NM-DOX&Tar, and AP-NM-DOX&Tar on MCF-7 cells after 24 h incubation. DOX concentration is varied from 0.3125 to 80 µg/mL. Mean ± SD (n = 3).

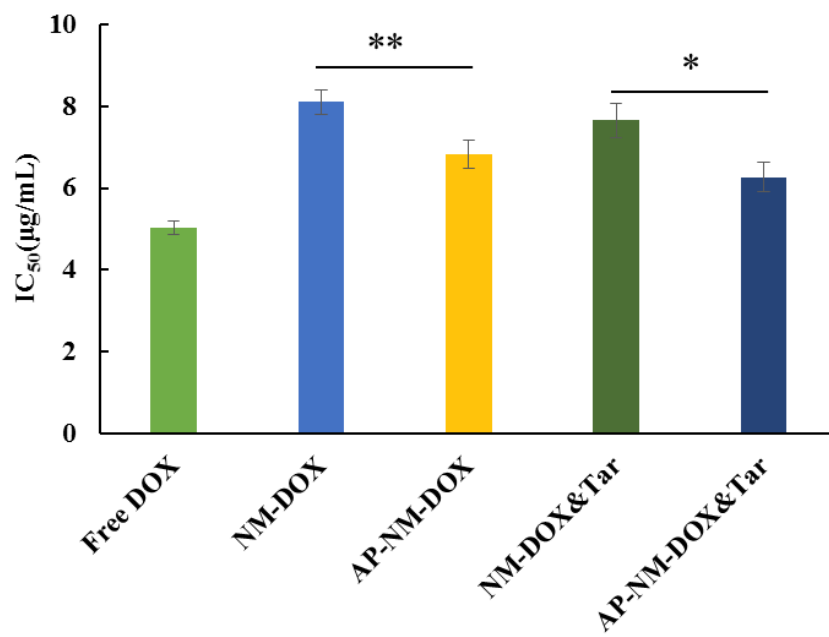


Figure S14 IC₅₀ value of different micelles on MCF-7 cells after 24 h incubation. Mean ± SD (n = 3). ** $p < 0.01$, * $p < 0.05$

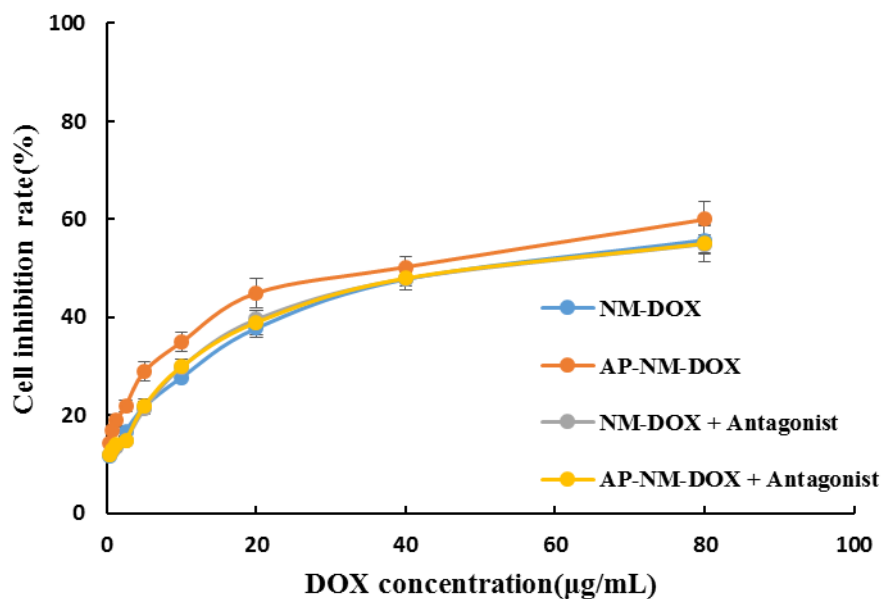


Figure S15 Inhibition effect of NM-DOX, AP-NM-DOX, NM-DOX + Antagonist, and AP-NM-DOX+Antagonist on MCF-7/ADR cells after 24 h incubation. DOX concentration is varied from 0.3125 to 80 µg/mL. Mean \pm SD (n = 3), Y₁R antagonist (CAS: 221697-09-2) was used at a dose of 10 µM.

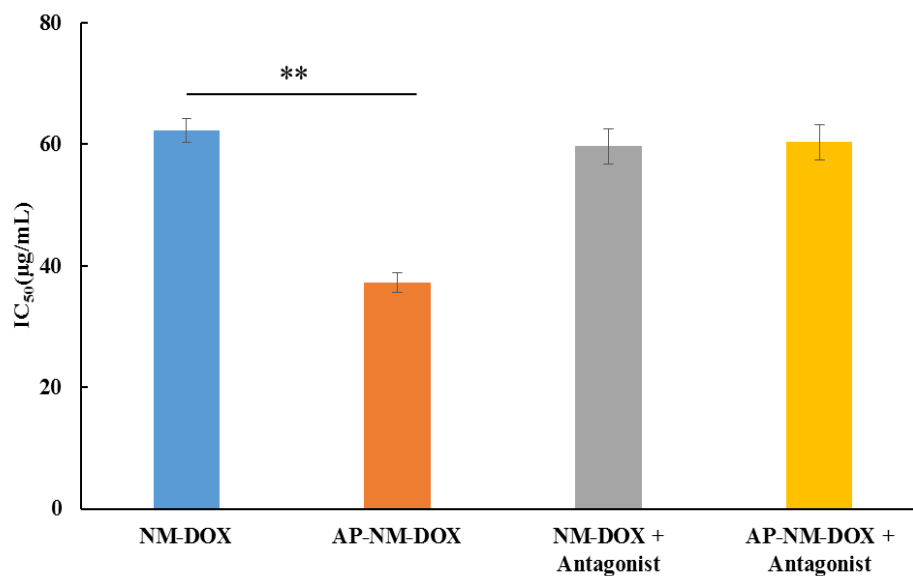


Figure S16 IC₅₀ value of different micelles of NM-DOX, AP-NM-DOX, NM-DOX+Antagonist, and AP-NM-DOX+Antagonist on MCF-7/ADR cells after 24 h incubation. DOX concentration is varied from 0.3125 to 80 µg/mL. Mean ± SD (n = 3), an antagonist of Y₁R (CAS: 221697-09-2) was used at a dose of 10 µM. ** $p < 0.01$

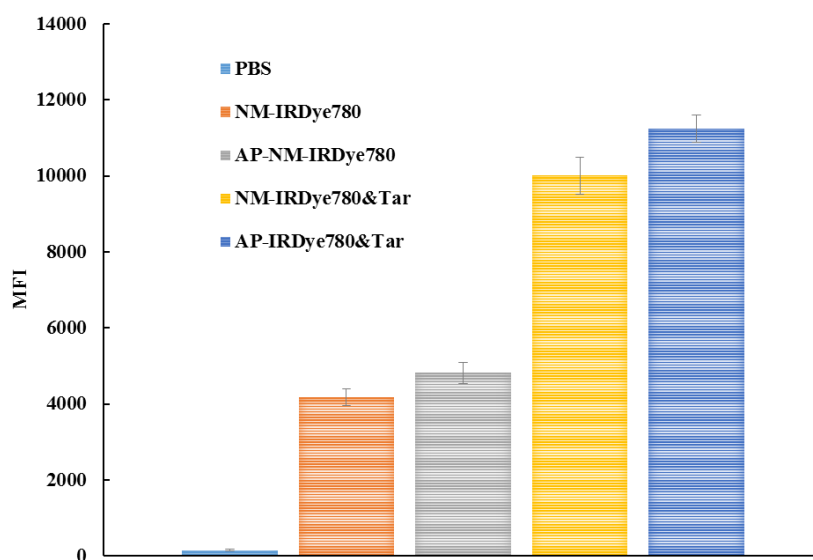


Figure S17 Mean fluorescence intensity (MFI) of MCF-7/ADR cells incubated with different IRDye780 loaded micelles following by flow cytometry analysis. All micelles were incubated with MCF-7/ADR cells for 8 h.

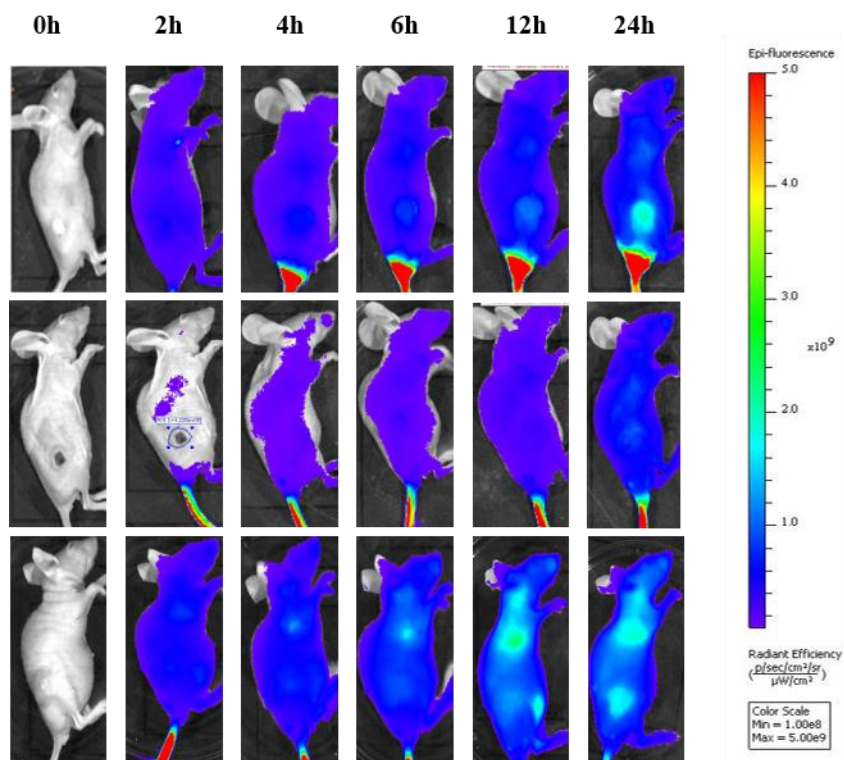


Figure S18 *In vivo* fluorescence imaging of MCF-7/ADR tumor bearing mice were taken before and after intravenous injection of NM-IRDye780 at 0, 2, 4, 6, 12, 24 h (IRDye780: 0.25 mg/kg).

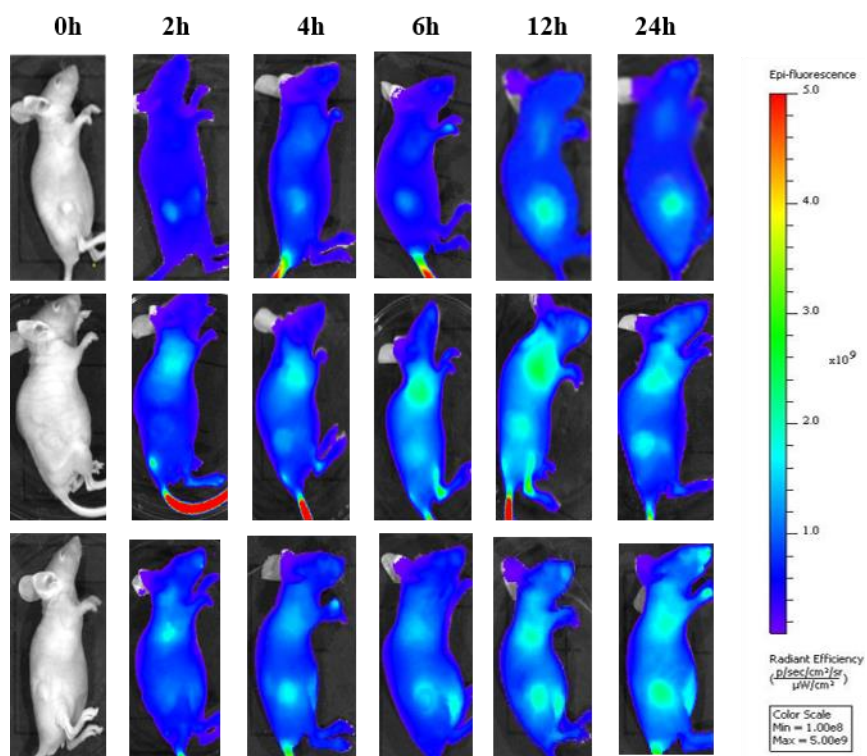


Figure S19 *In vivo* fluorescence imaging of MCF-7/ADR tumor bearing mice were taken before and after intravenous injection of AP-NM-IRDye780 at 0, 2, 4, 6, 12, 24 h (IRDye780: 0.25 mg/kg).

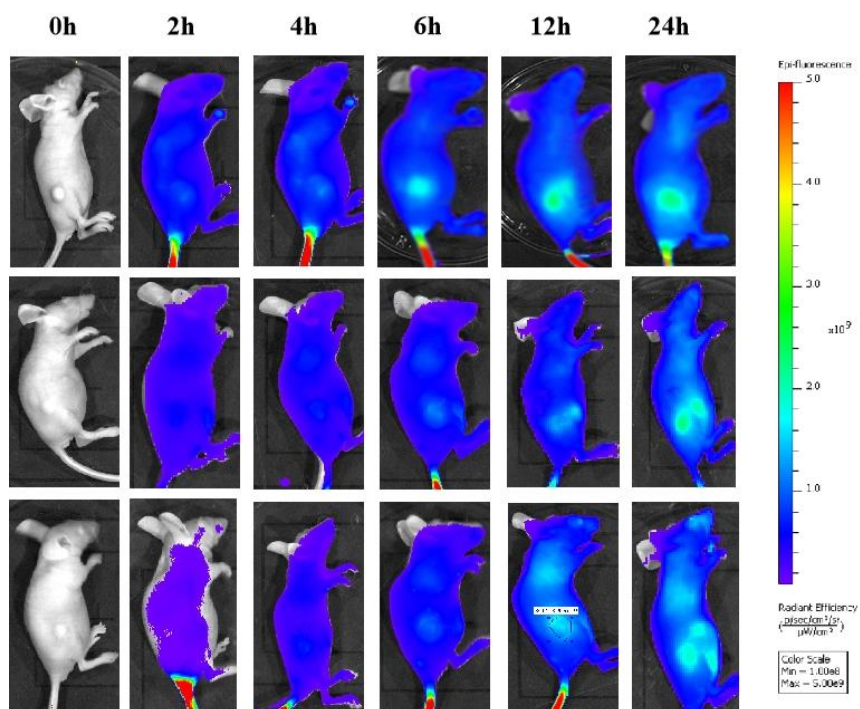


Figure S20 *In vivo* fluorescence imaging of MCF-7/ADR tumor bearing mice were taken before and after intravenous injection of NM-IRDye780&Tar at 0, 2, 4, 6, 12, 24 h (IRDye780: 0.25 mg/kg).

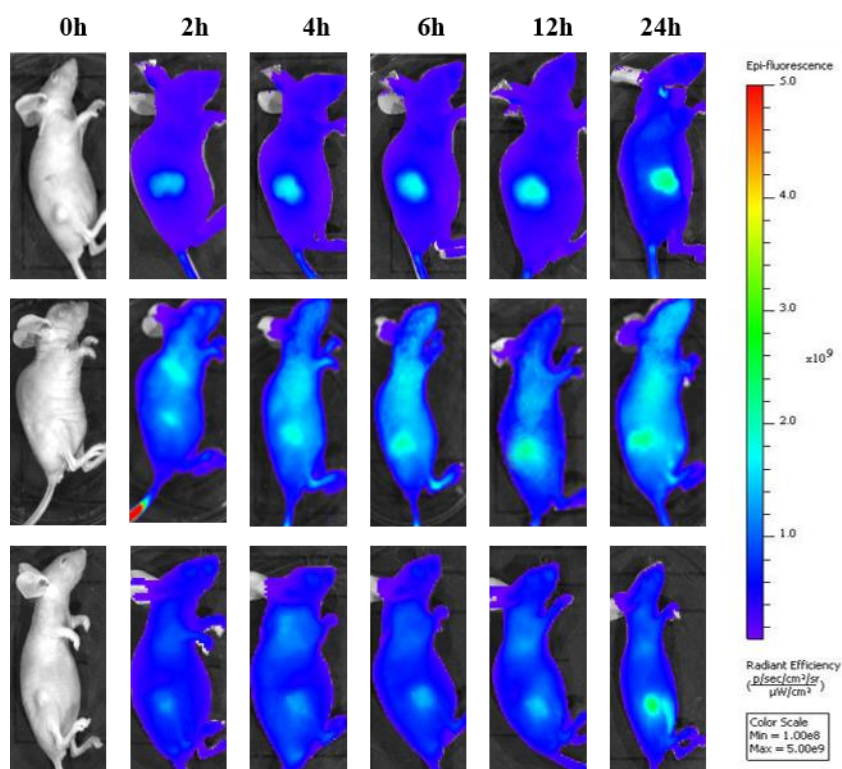


Figure S21 *In vivo* fluorescence imaging of MCF-7/ADR tumor bearing mice were taken before and after intravenous injection AP-NM-IRDye780&Tar at 0, 2, 4, 6, 12, 24 h (IRDye780: 0.25 mg/kg).

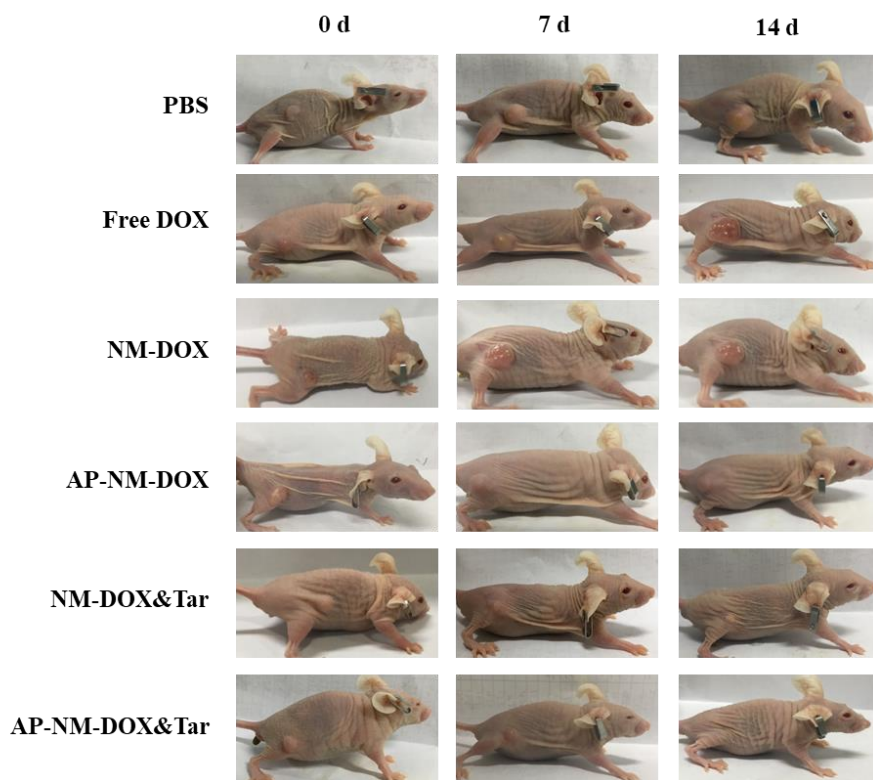


Figure S22 Photos of tumor-bearing mice after i.v. injection of PBS, free DOX, NM-DOX, AP-NM-DOX, NM-DOX&Tar, and AP-NM-DOX&Tar from 0 to 14 days.

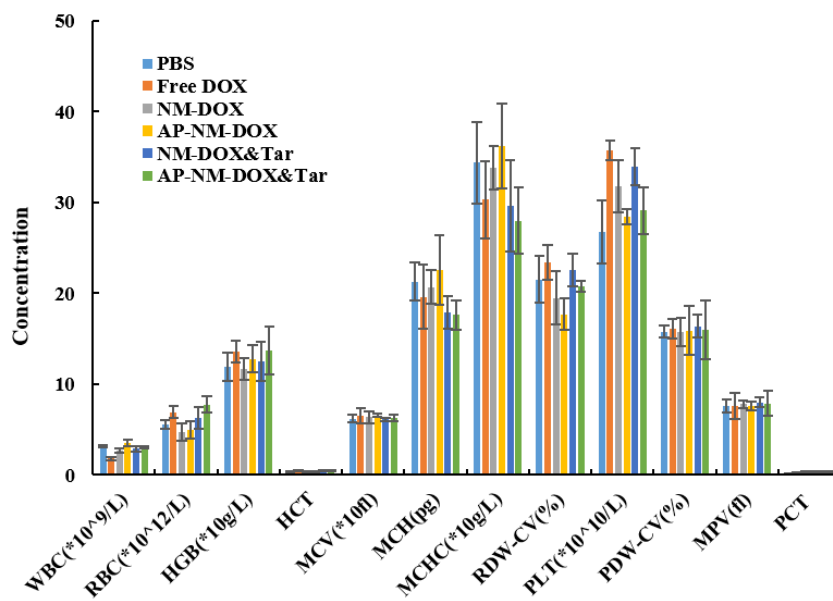


Figure S23 Hematological analysis of the mice after i.v. injection of PBS, free DOX, NM-DOX, AP-NM-DOX, NM-DOX&Tar, and AP-NM-DOX&Tar. Mean \pm SD (n = 3).

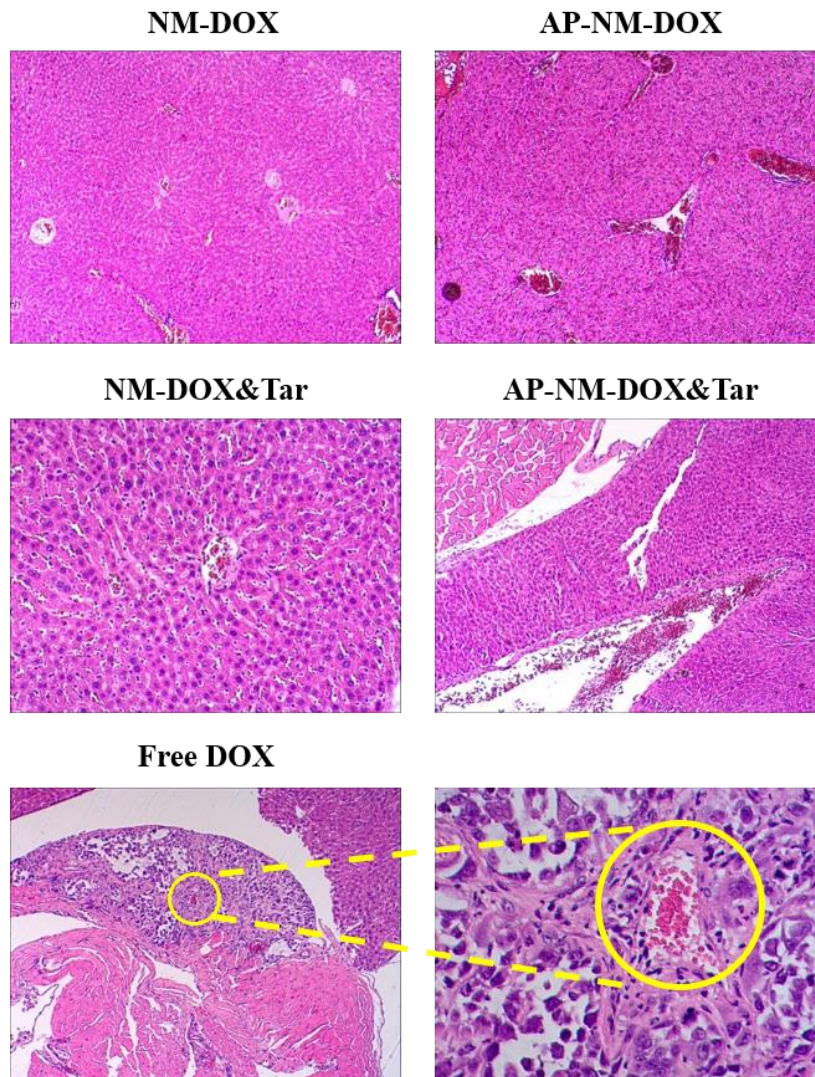


Figure S24 H&E staining of MCF-7/ADR tumor bearing nude mice liver after intravenous injection of Free DOX, NM-DOX, AP-NM-DOX, NM-DOX&Tar, and AP-NM-DOX &Tar. The mice were killed at 28th day after six times of tail vein injection.

Table S1 Characterization of nanomicelles

Sample name	Size (nm)	PDI	Zeta potential (mV)	DOX loading efficiency (%)	Tar loading efficiency (%)
NM-DOX	71.4 ± 3.1	0.189 ± 0.017	-9.8 ± 0.9	81.4 ± 1.1	--
AP-NM-DOX	60.9 ± 2.4	0.217 ± 0.014	-7.9 ± 0.8	82.3 ± 2.4	--
NM-DOX&Tar	74.5 ± 4.2	0.201 ± 0.009	-10.1 ± 0.6	86.9 ± 1.7	67.8 ± 2.3
AP-NM-DOX&Tar	82.1 ± 3.9	0.196 ± 0.008	-9.1 ± 1.3	87.1 ± 1.4	65.9 ± 1.8

1. L. Y. Zeng, Y. W. Pan, Y. Tian, X. Wang, W. Z. Ren, S. J. Wang, G. M. Lu and A. G. Wu, *Biomaterials*, 2015, **57**, 93-106.